University of Kentucky
UKnowledge

Spinal Cord and Brain Injury Research Center Faculty Publications

Spinal Cord and Brain Injury Research

4-2017

Carisbamate Blockade of T-Type Voltage-Gated Calcium Channels

Do Young Kim
Barrow Neurological Institute

Fang-Xiong Zhang
University of Calgary, Canada

Stan T. Nakanishi
University of Hawaii at Hilo

Timothy Mettler
Barrow Neurological Institute

Ik-Hyun Cho
Barrow Neurological Institute

See next page for additional authors

Right click to open a feedback form in a new tab to let us know how this document benefits you.

Follow this and additional works at: https://uknowledge.uky.edu/scobirc_facpub

Part of the Neurology Commons, and the Neuroscience and Neurobiology Commons

Authors

Do Young Kim, Fang-Xiong Zhang, Stan T. Nakanishi, Timothy Mettler, Ik-Hyun Cho, Younghee Ahn, Florian Hiess, Lina Chen, Patrick G. Sullivan, S. R. Wayne Chen, Gerald W. Zamponi, and Jong M. Rho

Carisbamate Blockade of T-Type Voltage-Gated Calcium Channels

Carisbamate Blockade of T-type Voltage-Gated Calcium Channels

Do Young Kim[*], **Fang-Xiong Zhang**[‡,§], **Stan T. Nakanishi**[†], **Timothy Mettler**[*], **Ik-Hyun Cho**[*], **Younghee Ahn**[#,¶], **Florian Hiess**[‡,‖], **Lina Chen**[‡], **Patrick G. Sullivan**[i], **S. R. Wayne Chen**[‡,‖], **Gerald W. Zamponi**[‡,§,Ⅎ], and **Jong M. Rho**[‡,#,¤,§,¶,Ⅎ]

[*]Departments of Neurology and Neurobiology, Barrow Neurological Institute, St. Joseph's Hospital & Medical Center, Phoenix, Arizona, USA

[‡]Department of Physiology and Pharmacology, University of Calgary, Calgary, Alberta, Canada

[#]Department of Pediatrics, University of Calgary, Calgary, Alberta, Canada

[¤]Department of Clinical Neurosciences, University of Calgary, Calgary, Alberta, Canada

[§]Hotchkiss Brain Institute, University of Calgary, Calgary, Alberta, Canada

[¶]Alberta Children's Hospital Research Institute, University of Calgary, Calgary, Alberta, Canada

[‖]Libin Cardiovascular Institute of Alberta, Cumming School of Medicine, University of Calgary, Calgary, Alberta, Canada

[†]Department of Biology, University of Hawai'i at Hilo, Hilo, Hawaii, USA

[i]Spinal Cord and Brain Injury Research Center, University of Kentucky, Lexington, Kentucky, USA

Summary

Objectives—Carisbamate (CRS) is a novel monocarbamate compound that possesses anti-seizure and neuroprotective properties. However, the mechanisms underlying these actions remain unclear. Here, we tested both direct and indirect effects of CRS on several cellular systems that regulate intracellular calcium $[Ca^{2+}]_i$.

Methods—We used a combination of cellular electrophysiological techniques, as well as cell viability, Store Overload-Induced Calcium Release (SOICR), and mitochondrial functional assays to determine whether CRS might affect release Ca^{2+} levels through actions on the endoplasmic reticulum (ER), mitochondria, and/or T-type voltage-gated Ca^{2+} channels.

Send Correspondence to: Jong M. Rho, MD, Section of Neurology, Alberta Children's Hospital, 2888 Shaganappi Trail, NW, Calgary, Alberta T3A 4N6 Canada, Tel: 403-955-2296; jong.rho@ahs.ca. Gerald W. Zamponi, PhD, FRSC, FCAHS, Senior Associate Dean for Research, Cumming School of Medicine, University of Calgary, 3330 Hospital Drive, NW, Calgary, T2N 4N1 Canada, Tel: 403-220-8687; zamponi@ucalgary.ca.
[Ⅎ]Co-Corresponding Authors

Results—In CA3 pyramidal neurons, kainic acid induced significant elevations in $[Ca^{2+}]_i$ and long-lasting neuronal hyperexcitability, both of which were reversed in a dose-dependent manner by CRS. Similarly, CRS suppressed spontaneous rhythmic epileptiform activity in hippocampal slices exposed to zero-Mg^{2+} or 4-AP. Treatment with CRS also protected murine hippocampal HT-22 cells against excitotoxic injury with glutamate, and this was accompanied by a reduction in $[Ca^{2+}]_i$ levels. Neither KA nor CRS alone altered the mitochondrial membrane potential (Ψ) in intact, acutely isolated mitochondria. Additionally, CRS did not affect mitochondrial respiratory chain activity, Ca^{2+}-induced mitochondrial permeability transition and Ca^{2+} release from the ER. However, CRS significantly decreased Ca^{2+} flux in HEK tsA-201 cells transfected with $Ca_v3.1$ (voltage-dependent T-type Ca^{2+}) channels.

Significance—Our data indicate that the neuroprotective and anti-seizure activity of CRS likely results in part from decreased $[Ca^{2+}]_i$ accumulation through blockade of T-type Ca^{2+} channels.

Introduction

Carisbamate (CRS; RWJ333369, (S)-2-O-carbamoyl-1-o-chlorophenyl-ethanol) is an investigational compound that has shown broad-spectrum efficacy against seizures in animal models and appears to exert neuroprotective effects.[1] Clinically, CRS has been shown to be effective and well tolerated in patients with refractory focal-onset seizures.[2,3] However, larger phase III clinical trial failed to document significant seizure reduction over the dose range studied.[4] Notwithstanding these results, CRS has recently been shown to enhance behavior and cognition in a model of TLE,[5] suggesting possible usefulness in controlling co-morbid symptoms of epilepsy.

While earlier studies have demonstrated CRS blockade of voltage-gated sodium channels and action potential firing in hippocampal neurons,[6,7] the mechanisms accounting for the beneficial effects of CRS remain unclear. Recently, CRS was found to decrease glutamate and increase glutamine brain levels in the rat lithium-pilocarpine model of TLE, but these effects were not consistently seen.[8] Further, electrophysiological studies indicated that CRS reduces glutamatergic transmission by an action potential-dependent presynaptic mechanism.[9] Given these observations, and the fact that neuronal hyperexcitability can arise from excessive intracellular calcium $[Ca^{2+}]_i$ accumulation, we asked whether CRS might alter Ca^{2+} homeostasis in hippocampal neurons, and tested both direct and indirect effects of CRS on the four major cellular systems that regulate calcium, namely cell membrane-bound glutamate receptors, voltage-gated calcium channels, mitochondria and the endoplasmic reticulum (ER).

Methods

All experimental procedures were approved by the respective institutional animal care and use committees (IACUCs) where the relevant studies were conducted: Barrow Neurological

Institute at St. Joseph's Hospital and Medical Center; the University of Kentucky (Lexington, KY, USA); and the University of Calgary (Calgary, Alberta, Canada).

Slice Electrophysiology

Male C3HeB/FeJ wild-type mice (4–7 weeks old) were anesthetized with isoflurane. Following decapitation, the brain was isolated and then submerged in ice-cold oxygenated physiological saline (124 mM NaCl, 1.8 mM $MgSO_4$, 4 mM KCl, 1.25 mM NaH_2PO_4, 26 mM $NaHCO_3$, 2.4 mM $CaCl_2$, and 10 mM D-glucose, [pH = 7.4]). Transverse hippocampal brain slices (300 μm) were cut using a vibratome and transferred to a perfusion chamber mounted on an Axioskop FS2 microscope (Carl Zeiss, Thornwood, NY, USA). Individual CA1 pyramidal neurons were visually identified under infrared-differential interference contrast (IR-DIC) optics. Tight-seal, whole-cell, patch-clamp recording was performed using borosilicate glass electrodes (4–7 MΩ) backfilled with an intracellular pipette solution composed of: 140 mM K-gluconate, 10 mM HEPES, 2 mM $MgCl_2$, 1 mM $CaCl_2$, 1 mM EGTA, and 2 mM K_2ATP, pH = 7.25).

Cell Culture and Transient Transfection

To study T-type calcium channels,[10] human $Ca_v3.1$ cDNA (Homo sapiens T calcium channel alpha 1G subunit variant 25, CACNA1G mRNA, complete cds, alternatively spliced) was expressed in tsA-201 human embryonic kidney (HEK) cells. HEK tsA-201 cells were grown to 80~90% confluence at 37°C (5% CO_2) in Dulbecco's modified Eagle's medium (Life Technologies, Grand Island, NY), supplemented with 10% (vol/vol) fetal bovine serum (HyClone, Thermo Scientific, Pittsburgh, PA), 200 U/ml penicillin, and 0.2 mg/ml streptomycin (Life Technologies, Grand Island, NY). Cells were suspended with 0.25% trypsin/ethylenediaminetetraacetic acid and plated onto glass coverslips in 10-cm culture dishes (Corning, Corning, NY) at 10% confluence 6 h before transfection. Calcium channel $Ca_v3.1$ (3 μg) and GFP marker (0.5 μg) DNAs were transfected into cells with calcium phosphate. Cells were transferred to 30°C 16–18 h later following transfection and stored for 2 days before recording.

Whole-Cell Electrophysiology

Cells on a glass coverslip were transferred into an external bath solution of 2 mM $CaCl_2$, 1 mM $MgCl_2$, 155 mM TEA-Cl, 2.5 mM 4-AP, 10 mM HEPES, 10 mM glucose, pH 7.4. Borosilicate glass pipettes (Sutter Instrument Co., Novato, CA) (3–5 MΩ) were filled with internal solution containing 140 mM CsCl, 2.5 mM $CaCl_2$, 1 mM $MgCl_2$, 5 mM EGTA, 10 mM HEPES, 2 mM Na-ATP and 0.3 mM Na-GTP, pH 7.3. Whole-cell patch clamp recordings were performed by using an EPC 10 amplifier (HEKA Elektronik, Bellmore, NY) linked to a personal computer equipped with Pulse (V8.65) software (HEKA Elektronik). After seal formation, the membrane beneath the pipette was ruptured and the pipette solution was allowed to dialyze into the cell for 2–5 min before recording. Voltage-dependent currents were leak corrected with an online P/4 subtraction paradigm. Data were recorded at 10 kHz and filtered at 2.9 kHz. T-type calcium currents were elicited by depolarization from a holding potential of -110 mV to a test potential of −20 mV with an interpulse interval of 20 s. The duration of the test pulse was typically 40 ms. In current-voltage relation studies for $Ca_v3.1$, the membrane potential was held at −110 mV and cells

were depolarized from −60 to +60 mV in 5 mV increments. In steady-state inactivation studies for Cav3.1, a 3 sec conditioning prepulse of various magnitudes (initial holding at −110 mV) was followed by a depolarizing pulse to −20 mV. Individual sweeps were separated by 12 s to permit recovery from inactivation between conditioning pulses. The current amplitude obtained from test pulse was normalized to that observed at the holding potential of −110 mV.

Data analysis was performed by using online analysis built in Pulse software (HEKA Elektronik), and all graphs and curve fittings were prepared by using GraphPad Prism 5 (GraphPad Software, La Jolla, CA). Dose–response curves were fitted with the equation $y = A_2 + (A_1 - A_2)/(1 + ([C]/IC_{50})^n)$, where A_1 is initial current amplitude and A_2 is the current amplitude at saturating drug concentrations, [C] is the drug concentration, and n is the Hill coefficient. Current–voltage relationships were fitted with the modified Boltzmann equation: $I = [G_{max}(V_m - E_{rev})]/[1 + \exp((V_{0.5act} - V_m)/\kappa_a)]$, where V_m is the test potential, $V_{0.5act}$ is the half activation potential, E_{rev} is the reversal potential, G_{max} is the maximum slope conductance, and κ_a reflects the slope of the activation curve. Steady-state inactivation curves were fitted using the Boltzmann equation: $I = 1/(1 + \exp((V_m - V_h)/\kappa))$, where V_h is the half-inactivation potential and κ is the slope factor.

Calcium imaging and cell viability assay

Hippocampal slices were incubated with the calcium indicator dye Fura2-AM (10 μM; Invitrogen) for 1 hour. Each slice was transferred to a recording chamber fixed to an Axioskop FS2 IR-DIC microscope outfitted with the Zeiss Stallion 2 imaging system. Ratiometric fluorescence intensities in regions of interest were then recorded using a 340 nm/380 nm excitation filter set controlled by a high-speed filter switching device. Photometric changes in fluorescence intensity (indicating alterations in free cytosolic $[Ca^{2+}]$), were recorded before, during and after drug applications from CA3 pyramidal neurons every 10 sec.

To assess calcium release from the endoplasmic reticulum (ER), HEK293 cells were transfected with ryanodine receptor 2 (RyR2) cDNA using Ca^{2+} phosphate precipitation, and intracellular Ca^{2+} dynamics were measured as described previously.[11] Briefly, transfected HEK293 cells were grown on glass coverslips for up to 24 hr, and then loaded with Fura2-AM (5 μM) in KRH (Krebs-Ringer-HEPES) buffer (125 mM NaCl, 5 mM KCl, 1.2 mM KH_2PO_4, 6 mM glucose, 1.2 mM $MgCl_2$ and 25 mM HEPES [pH = 7.4]) with 0.02% Pluronic F-127 and 0.1 mg/ml BSA for 20 min at room temperature (23 °C). Coverslips with dye-loaded HEK293 cells were then transferred to a perfusion chamber on an inverted microscope (Nikon TE2000-S). The chamber was constantly perfused with KRH buffer containing 2 mM Ca^{2+}, and time-lapse images (0.5 frames/sec) were recorded on a PC and stored for offline analysis of fluorescence intensity using Compix Simple PCI 6 software (Compix Inc., Cranberry Township, PA, USA). Bath application of 2 mM Ca^{2+} evoked an oscillatory store Overload-Induced Calcium Release (SOICR) from the ER of HEK293 cells, and the resulting changes in fluorescence intensity were used to quantify the amplitude and frequency of the SOICR.

Neuroprotection Assays

Murine hippocampal HT-22 cells were cultured with Dulbecco's Modified Eagle Medium (DMEM) supplemented with 10% fetal bovine serum (FBS), 100 U/mL penicillin, and 100 mg/mL streptomycin. HT-22 cells were seeded in 96-well cell culture plates (5,000 cells per well) and grown overnight. Cells were then treated with either media alone or CRS followed by the addition of glutamate. After a 24-hr incubation, HT-22 cells were washed with PBS and loaded with 10 μM Fura2-AM for 1 hr at 37°C. Loaded cells were washed twice with DPBS, and the intracellular calcium level was measured with a plate reader by successive excitation of 340 nm and 380 nm. The emitted fluorescence was passed through a 510 nm filter. Quantification of the $[Ca^{2+}]$ was achieved by averaging the ratio of fluorescent signal acquired at 340 nm and 380 nm. To measure changes in cell survival against glutamate, 20 μl of 3-(4,5-dimethylthiazol-2-yl)-2,5-diphenyltetrazolium bromide (MTT; 2.5 mg/mL) was added to the wells and incubated for 3 hr. After incubation, the media was removed from the wells and 100 μL of dimethylsulfoxide (DMSO) was added to dissolve the formazan reagent. The absorbance was read using an Infinite m200 pro (TEKAN) reader at 565 nm. Cell viability was expressed as a percentage of the control group.

Mitochondrial isolation and mitochondrial membrane potential (Ψ) measurements

Our procedures were modified from previously described protocols.[12] Isolated brains were homogenized in isolation buffer and subsequently centrifuged at 1,300 g for 3 min at 4°C. The isolated supernatant was centrifuged at 13,000 g for 10 min at 4 °C. The collected pellet was re-suspended in 1.5 ml of isolation buffer with 0.01% digitonin and then centrifuged at 10,000 g for 10 min at 4°C. The pellet was re-suspended in 500 μl of isolation buffer. For Ficoll purification, the gradient was made by first loading the Ficoll 10% solution in the ultracentrifuge tube and then adding the Ficoll 7.5% solution. Loaded samples on top of the Ficoll gradient were centrifuged at 32,000 g for 30 min at 4°C. The collected pellet was re-suspended in isolation buffer without EGTA and spun at 10,000 g for 10 min at 4°C. The pellet was again re-suspended in isolation buffer without EGTA, and then protein concentration was determined by a BCA protein assay kit.

 Ψ was measured using the dye 5,5′,6,6′-tetrachloro-1,1′,3,3′-tetraethylbenzimidazolyl carbocyanine iodide (MitoPT^{TM}-JC1 kit; ImmunoChemistry Technologies). JC-1 emits green fluorescence at a low membrane potential (Ψ disruption), whereas polarized mitochondrial potentials reversibly form red fluorescent "J-aggregates" (Ψ stabilization). Briefly, aliquots of 250 μg of isolated mitochondrial protein were suspended in KCl respiration buffer (125 mM KCl, 2 mM MgCl, 2.5 mM KH$_2$PO$_4$, 20mM HEPES, and 0.1% BSA [pH 7.2]) mixed with tested drugs and 10 μM JC-1 to make a final volume of 200 μL and then incubated at 37°C for 30 min. Fluorescence intensity was measured with a TECAN SpectraFluor Microplate Reader (TECAN) under excitation and emission wavelengths of 485 nm and 595 nm, respectively. Here, changes in red fluorescence intensities were indicative of Ψ and compared to the control optical density (OD) values.

Spectrofluorophotometer assays

Fractions enriched in mitochondria (200 μg protein/mL) were placed in 2 mL of KCl respiration buffer within a temperature-controlled cuvette at 37°C with 100 nM CaG5 N

(excitation 506 nm, emission 532 nm; to monitor extra-mitochondrial Ca^{2+}) and 150 nM TMRE (excitation 550 nm, emission 575 nm; to monitor change in the mitochondrial membrane potential, Ψ_m) in a Shimadzu RF-5301PC spectrofluorophotometer (Shimadzu, Tokyo, Japan). Each time-scan began with a baseline reading followed by the addition of 5 mmol/L pyruvate and 2.5 mmol/L malate at 1 min, 150 μmol/L ADP at 2 min, and 1 μmol/L oligomycin at 3 min. At 5 min, Ca^{2+} was added via an infusion syringe pump (80 nmol Ca^{2+}/mg protein per minute) until the mitochondria were no longer able to buffer the added Ca^{2+}. The chemical uncoupler, FCCP (1 μM; carbonyl cyanide-p-trifluoromethoxyphenylhydrazone), was added toward the end of the each run. The recorded traces, representative of at least three separate independent experiments, were quantified by calculating the average baseline CaG5 N fluorescence readings 1 min prior to the beginning of the Ca^{2+} infusion using the Shimadzu Hyper RF software (Shimadzu) and Microsoft Excel. The time-point at which the CaG5 N signal was 150% above the average baseline reading was considered the point at which mitochondria were overloaded and no longer capable of removing Ca^{2+} from the media, indicating onset of mitochondrial permeability transition (mPT).

Drugs and statistical analysis

All reagents used in this study were purchased from Sigma-Aldrich (St. Louis, MO, USA) unless otherwise stated. Carisbamate (CRS) was obtained as a gift from Johnson & Johnson Pharmaceuticals and was dissolved in dimethylsulfoxide (DMSO) at various concentrations (but did not exceed 0.1%). Numerical data are expressed as the mean ± SEM. Student t-test or ANOVA was performed to determine differences among experimental groups, with significance set at $p < 0.05$.

Results

Carisbamate inhibits kainic acid-evoked epileptiform activity in vitro

First, we assessed whether CRS diminishes kainic acid (KA)-evoked neuronal excitability in CA3 pyramidal neurons using acute hippocampal slices. Bath application of 10 μM KA induced long-lasting hyperexcitable changes superimposed on membrane depolarization (20 out of 20 cells; Fig. 1A,D). Upon application of KA in cells pretreated with 100 μM CRS, 8 out of 20 cells did not exhibit neuronal hyperexcitability. This effect was sustained up to 20 min after washout (Fig. 1B,C,D). The attenuation of sustained action potential discharge was more pronounced with 300 μM CRS (22 out of 30 cells; Fig. 1C,D).

The inhibitory effects of CRS were also examined with either Mg^{2+}-free physiological saline (which alleviates the Mg^{2+} block of N-methyl-D-aspartate [NMDA] receptors) or 300 μM 4-aminopyridine (4-AP; a non-selective K^+ channel blocker and Ca^{2+} channel activator). Under both of these experimental conditions, spontaneous rhythmic epileptiform discharges were seen, characterized by sustained over-riding action potentials (Fig. 1E). Consistent with anti-seizure effects previously seen in cortical slices,[6] CRS (300 μM) blocked epileptiform discharges in both of these models (n = 7 cells/each study; Fig. 1E).

CRS reduces KA-mediated intracellular Ca^{2+} influx

Given our initial results and prior literature showing increases in $[Ca^{2+}]_i$ following glutamate receptor activation,[13,14] we tested whether CRS could prevent elevations of $[Ca^{2+}]_i$ after KA exposure using the intracellular Ca^{2+} indicator dye Fura2-AM. CRS did not alter the baseline fluorescence ratio ($F_{340/380}$) when applied alone, whereas KA resulted in an immediate increase in $[Ca^{2+}]_i$ in CA3 pyramidal neurons (n = 12; Fig. 2A). Consistent with our initial electrophysiological findings, pre-treatment with 300 μM CRS produced a substantial reduction in $[Ca^{2+}]_i$ compared to cells treated solely with KA (n = 12; Fig. 2A).

We also reasoned that CRS would induce suppressive effects on zero-Mg^{2+}-evoked epileptiform discharges. To confirm this, we measured glutamate-mediated $[Ca^{2+}]_i$ accumulation in murine hippocampal HT-22 cells with and without CRS using Fura2-AM. In these cells, CRS alone (10 and 100 μM) had no influence on $[Ca^{2+}]_i$ levels, but both 5 mM and 10 mM glutamate dose-dependently increased the level of $[Ca^{2+}]_i$ compared to HT-22 cells exposed only to media (Fig. 2B). When 5 mM glutamate was co-applied with either 10 μM or 100 μM CRS, the $[Ca^{2+}]_i$ level declined significantly by 19% (117 ± 5, n = 10) and 33% (104 ± 5.7, n = 10), respectively, compared to cells treated with 5 mM glutamate alone (136 ± 3.2, n = 10). No differences were seen with media alone, compared to 100 μM CRS plus 5 mM glutamate. At 10 mM glutamate (along with either 10 μM or 100 μM CRS), $[Ca^{2+}]_i$ levels were significantly reduced by 40% (131 ± 7.5, n = 10) and 54% (117 ± 6, n = 10), respectively, compared to cells treated with 10 mM glutamate alone (171 ± 6, n = 10) (Fig. 2B). These data further support the notion that CRS contributes to an anti-seizure action by decreasing pathological $[Ca^{2+}]_i$ influx.

CRS prevents glutamate-induced neuronal injury

Next, we sought to determine whether the reduction in $[Ca^{2+}]_I$ by CRS could be correlated with morphological neuroprotection. Using a live-cell imaging system, HT-22 cells exposed to 500 μM glutamate alone for 24 hr resulted in a 40% decrease in cell viability (Fig. 3A). However, cells treated concomitantly for 1 hr with 100 μM CRS and 500 μM glutamate appeared healthy. 100 μM CRS alone had no influence on cell survival (Fig. 3B).

CRS does not affect ER- or mitochondria-mediated changes in $[Ca2+]_i$

While neuronal hyperexcitability involves increased accumulation of $[Ca^{2+}]_i$, prolonged depolarization also triggers the release of Ca^{2+} from the ER through inositol 1,4,5-trisphosphate (IP_3) and ryanodine receptors.[15] Further, aberrant $[Ca^{2+}]_i$ overloading can arise from mitochondrial dysfunction, such as the disruption of mitochondrial membrane potential (ψ) and mitochondrial permeability transition (mPT) opening.[16,17] Irrespective of the actual causes of pathological rises in $[Ca^{2+}]_i$, the net effect is activation of cell death cascade.[14]

Given the important role of the ER and mitochondria in regulating intracellular calcium levels, we asked whether CRS might affect either one or both of these organelles and processes regulating intracellular calcium homeostasis. It has been shown that store Ca^{2+} overload can trigger spontaneous Ca^{2+} oscillations (store overload-induced Ca^{2+} release, or SOICR) via the ryanodine receptor.[18] We next determined the impact of CRS on SOICR.

There were no differences amongst groups treated with various CRS doses compared to controls, with respect to either the amplitude or frequency (n = 3–5 for each dose; Fig. 4A). However, the SOICR amplitude in the 1 mM CRS-treated group was significantly lower compared to that seen when lower doses of CRS and DMSO (control) were used (Fig. 4B, $p < 0.05$); however, SOICR frequency was not changed with 1 mM CRS administration.

Next, we explored a potential modulatory effect of CRS on the mitochondrial membrane potential (ψ) or Ca^{2+}-induced mPT. Acutely isolated hippocampal mitochondria were prepared, and exposed to CRS. We monitored the change in ψ from JC1-loaded isolated mitochondria treated with either 10 μM KA or 300 μM CRS for 30 min. Neither KA nor CRS separately altered ψ. In contrast, application of 100 nM rotenone (Rot), a toxic compound that acts by inhibiting Complex I of the electron transport chain, triggered a significant decrease in Ψ (Fig. 5A, $p < 0.01$) as previously reported,[19] but 300 μM CRS had no effect on the Rot-evoked Ψ depolarization (Fig 5A). Given that a potential pathological correlation exists between calcium overloading and mPT activation, we then asked whether CRS can regulate Ca^{2+}-induced mPT. We found that CRS alone did not affect the threshold for Ca^{2+}-induced mPT opening (Fig. 5B,C).

CRS inhibits T-type Ca^{2+} channels

In the genetic absence epilepsy rat of Strasbourg (GAERS) model, CRS was found to strongly suppress spike-wave-discharges.[20] While there are many drugs that exhibit similar effects, the prototypic agent and first-line therapy for absence epilepsy, ethosuximide, is known to block low-threshold, T-type Ca^{2+} channels which play a pivotal role in the genesis of absence seizures in the thalamocortical network.[21–24] To investigate the possibility that CRS interacts with T-type Ca^{2+} channels, we performed whole-cell recordings in tsA-201 HEK cells expressing $Ca_v3.1$ channels. Fast-inactivating T-type currents, generated by recombinant $Ca_v3.1$ channels, were generated in response to depolarizing pulses (Fig. 6). With infusion of 100 μM CRS, a reduction in the T-type current was seen, with a peak effect when depolarized from –110 mV to –30 mV (Fig. 6A,B). The current-voltage relationship of T-type Ca^{2+} channel in response to CRS under different voltage steps revealed a significant decrease in whole-cell current amplitude across a wide range of voltages (Fig. 6C). There was a significant shift in the half-inactivation potential upon application of 300 μM CRS (Fig. 6D), indicating that this compound is able to stabilize the inactivated state of the channel. Importantly, this shift resulted in further inhibition of whole-cell current amplitudes at more depolarized membrane potentials. In additional experiments, we found no modulatory effects of 100 μM and 300 μM CRS on HEK cells transfected with $Ca_v3.2$ channels (n = 3; data not shown). Collectively, these results support our notion that the T-type Ca^{2+} channel – specifically, the $Ca_v3.1$ isoform – is a target of CRS action, and may play an important role in regulating not only intracellular Ca^{2+} but importantly, the anti-seizure and neuroprotective effects seen with this novel anti-seizure medication.

Discussion

In the present study, we show that CRS can inhibit KA-induced neuronal hyperexcitability, elevations in $[Ca^{2+}]_i$, and subsequent hippocampal cell death in a dose-dependent manner.

While a direct mechanistic link to ryanodine receptors or to mitochondrial function could not be established, we nevertheless found that a clinically relevant concentration, CRS (300 µM) was able to significantly attenuate T-type Ca^{2+} currents in HEK cells transfected with recombinant $Ca_v3.1$ channels. Thus, after evaluating several major sources of calcium influx into the cell, we conclude from our data that the anti-seizure and morphological neuroprotective effects of CRS are likely due in part to blockade of T-type Ca^{2+} channels.

It is well known that KA-induced epileptogenesis is associated with activation of voltage-dependent calcium channels[25,26] which contributes to neuronal hyperexcitability and subsequent cell death.[13,27] Our current findings are in keeping with the extensive prior literature, and more specifically with *in vivo* and *in vitro* experiments wherein CRS was demonstrated to reduce seizure activity induced by KA.[28] Blockade of T-type calcium current constitutes a possible mechanism of action of CRS that augments inhibition of voltage-gated Na^+ channels, as evidenced by earlier studies revealing CRS's ability to decrease membrane input resistance and diminish action potential firing.[6,7]

With respect to neuronal injury, prolonged elevation in $[Ca^{2+}]_i$ following the activation of glutamate receptors is widely accepted as a key factor in the processes of both neuronal injury and epileptogenesis.[29] In this regard, our findings in the *in vitro* zero-Mg^{2+} model (Fig. 1E) are also consistent with the linkage between "seizure-like" epileptiform discharges and glutamate receptor-mediated calcium influx.[30] Further, we show that CRS was able to exert effects against glutamate, similar to what was seen with KA exposure, specifically a normalization of $[Ca^{2+}]_i$ levels (Fig. 2). This is consistent with the previously demonstrated inhibition of "seizure-like" rhythmic discharges in hippocampal slices bathed in zero-Mg^{2+} aCSF.[6,31]

Excessive glutamate (specifically, NMDA) receptor activation, while impairing $[Ca^{2+}]_i$ homeostasis, can also facilitate release of Ca^{2+} through ryanodine receptors (RyRs) from the ER.[32] While there are compelling data that CRS can suppress glutamate-mediated synaptic transmission in the granule cells of the dentate gyrus,[9] we could not confirm a direct effect of CRS on RyRs in the ER. However, it is likely that the inhibitory action of CRS on glutamate neurotransmission and blockade of T-type Ca^{2+} channels can secondarily reduce the calcium burden on the ER.

The other major organelle to consider when studying intracellular calcium homeostasis is the mitochondrion. There is abundant evidence that mitochondria can act as a Ca^{2+} buffer under conditions of NMDA-evoked increases in $[Ca^{2+}]_i$, thereby helping to prevent neuronal injury or death.[33] However, when cellular homeostatic and compensatory systems fail to contain pathological rises in $[Ca^{2+}]_i$, or when excessive mitochondrial Ca^{2+} accumulation occurs, cell death pathways are triggered via depolarization of ψ and opening of the mitochondrial permeability transition pore.[16,17] In the present study, activation of kainate receptors elevated $[Ca^{2+}]_i$ in CA3 pyramidal neurons, but KA alone was unable to alter ψ in isolated mitochondria, suggesting that the pharmacological actions of KA are likely upstream of the mitochondrion. Similarly, neither ψ nor Ca^{2+}-induced mPT opening was affected after exposure to CRS. Despite the lack of direct interaction of CRS on mitochondria, we cannot

exclude the possibility that the upstream modulation of $[Ca^{2+}]_i$ influx by CRS reduces overall mitochondrial Ca^{2+} accumulation.

It is well established that T-type Ca^{2+} channels are critically involved in absence seizures [33–37] and that specific blockers of $Ca_v3.1$ exert anti-seizure activity in both humans and animal models.[37,38] Consistent with these data, we observed that $Ca_v3.1$ (but not $Ca_v3.2$) Ca^{2+} currents were significantly attenuated by clinically relevant concentrations of CRS. We did not, however, evaluate the effects of CRS on high voltage-activated (HVA) calcium channels, as an earlier study indicated that selective HVA blockers were unable to reverse the inhibitory effect of CRS on α-amino-3-hydroxy-5-methyl-4-isoxazolepropionic acid (AMPA)-mediated excitatory post-synaptic currents.[9] Curiously though, unlike the prototypic T-type calcium channel blocker ethosuximide, CRS appears to have greater broad-spectrum activity in multiple animal models of seizures and epilepsy,[39] suggesting other yet undefined mechanisms of action.[8,9] To this point, CRS has been shown to inhibit glutamatergic neurotransmission in the dentate gyrus through an action potential-dependent mechanism, but not through pre-synaptic calcium channels.[9]

In summary, we provide evidence that the anti-seizure and neuroprotective effects of CRS may be explained partly on the basis of its ability to block T-type calcium channels in neurons, and also by preventing excessive intracellular calcium accumulation such as would occur through glutamate receptor activation. CRS also inhibits voltage-gated sodium channels, and there is recent evidence that this novel monocarbamate compound can modulate the activation of a GABA-mediated chloride conductance.[6,7] Thus, with growing evidence that CRS may afford functional and neuroprotective – as well as disease-modifying – effects beyond epilepsy, the greater elucidation of basic mechanisms underlying these actions may lead to the development of analog compounds having similar profiles.

Acknowledgments

References

1. Francois J, Germe K, Ferrandon A, et al. Carisbamate has powerful disease-modifying effects in the lithium-pilocarpine model of temporal lobe epilepsy. Neuropharmacology. 2011; 61:313–328. [PubMed: 21539848]

2. Faught E, Holmes GL, Rosenfeld WE, et al. Randomized, controlled, dose-ranging trial of carisbamate for partial-onset seizures. Neurology. 2008; 71:1586–1593. [PubMed: 19001248]

3. Sperling MR, Greenspan A, Cramer JA, et al. Carisbamate as adjunctive treatment of partial onset seizures in adults in two randomized, placebo-controlled trials. Epilepsia. 2010; 51:333–343. [PubMed: 19863578]

4. Halford JJ, Ben-Menachem E, Kwan P, et al. A randomized, double-blind, placebo-controlled study of the efficacy, safety, and tolerability of adjunctive carisbamate treatment in patients with partial-onset seizures. Epilepsia. 2011; 52:816–25. [PubMed: 21320109]

5. Faure JB, Akimana G, Carneiro JE, et al. A comprehensive behavioral evaluation in the lithium-pilocarpine model in rats: effects of carisbamate administration during status epilepticus. Epilepsia. 2013; 54:1203–1213. [PubMed: 23663139]

6. Whalley BJ, Stephens GJ, Constanti A. Investigation of the effects of the novel anticonvulsant compound carisbamate (RWJ-333369) on rat piriform cortical neurones in vitro. Br J Pharmacol. 2009; 156:994–1008. [PubMed: 19226287]

7. Liu Y, Yohrling GJ, Wang Y, et al. Carisbamate, a novel neuromodulator, inhibits voltage-gated sodium channels and action potential firing of rat hippocampal neurons. Epilepsy Res. 2009; 83:66–72. [PubMed: 19013768]

8. Hadera MG, Faure JB, Berggaard N, et al. The anticonvulsant actions of carisbamate associate with alterations in astrocyte glutamine metabolism in the lithium-pilocarpine epilepsy model. J Neurochem. 2014; 132:532–545. [PubMed: 25345404]

9. Lee CY, Lee ML, Shih CC, et al. Carisbamate (RWJ-333369) inhibits glutamate transmission in the granule cell of the dentate gyrus. Neuropharmacology. 2011; 61:1239–1247. [PubMed: 21824485]

10. Bladen C, Zamponi GW. Common mechanisms of drug interactions with sodium and T-type calcium channels. Mol Pharmacol. 2012; 82:481–487. [PubMed: 22695716]

11. Chen W, Wang R, Chen B, et al. The ryanodine receptor store-sensing gate controls Ca2+ waves and Ca2+-triggered arrhythmias. Nat Med. 2014; 20:184–192. [PubMed: 24441828]

12. Kim DY, Davis LM, Sullivan PG, et al. Ketone bodies are protective against oxidative stress in neocortical neurons. J Neurochem. 2007; 101:1316–1326. [PubMed: 17403035]

13. Berg M, Bruhn T, Frandsen A, et al. Kainic acid-induced seizures and brain damage in the rat: role of calcium homeostasis. J Neurosci Res. 1995; 40:641–646. [PubMed: 7602615]

14. Choi DW. Glutamate neurotoxicity and diseases of the nervous system. Neuron. 1988; 1:623–634. [PubMed: 2908446]

15. Ruiz A, Matute C, Alberdi E. Endoplasmic reticulum Ca(2+) release through ryanodine and IP(3) receptors contributes to neuronal excitotoxicity. Cell Calcium. 2009; 46:273–281. [PubMed: 19747726]

16. Dubinsky JM, Levi Y. Calcium-induced activation of the mitochondrial permeability transition in hippocampal neurons. J Neurosci Res. 1998; 53:728–741. [PubMed: 9753200]

17. Kovacs R, Kardos J, Heinemann U, et al. Mitochondrial calcium ion and membrane potential transients follow the pattern of epileptiform discharges in hippocampal slice cultures. J Neurosci. 2005; 25:4260–4269. [PubMed: 15858052]

18. Chen W, Wang R, Chen B, et al. The ryanodine receptor store-sensing gate controls Ca2+ waves and Ca2+-triggered arrhythmias. Nat Med. 2014; 20:184–192. [PubMed: 24441828]

19. Barrientos A, Moraes CT. Titrating the effects of mitochondrial complex I impairment in the cell physiology. J Biol Chem. 1999; 274:16188–16197. [PubMed: 10347173]

20. Francois J, Boehrer A, Nehlig A. Effects of carisbamate (RWJ-333369) in two models of genetically determined generalized epilepsy, the GAERS and the audiogenic Wistar AS. Epilepsia. 2008; 49:393–399. [PubMed: 17822432]

21. Gomora JC, Daud AN, Weiergraber M, et al. Block of cloned human T-type calcium channels by succinimide antiepileptic drugs. Mol Pharmacol. 2001; 60:1121–1132. [PubMed: 11641441]

22. Pinault D, Leresche N, Charpier S, et al. Intracellular recordings in thalamic neurones during spontaneous spike and wave discharges in rats with absence epilepsy. J Physiol. 1998; 509:449–456. [PubMed: 9575294]

23. Slaght SJ, Leresche N, Deniau JM, et al. Activity of thalamic reticular neurons during spontaneous genetically determined spike and wave discharges. J Neurosci. 2002; 22:2323–2334. [PubMed: 11896171]

24. Meis S, Biella G, Pape HC. (1996) Interaction between low voltage-activated currents in reticular thalamic neurons in a rat model of absence epilepsy. Eur J Neurosci. 1996; 8:2090–2097. [PubMed: 8921300]

25. Murphy SN, Thayer SA, Miller RJ. The effects of excitatory amino acids on intracellular calcium in single mouse striatal neurons in vitro. J Neurosci. 1987; 7:4145–4158. [PubMed: 3320284]

26. Hoyt KR, Stout AK, Cardman JM, et al. The role of intracellular Na+ and mitochondria in buffering of kainate-induced intracellular free Ca2+ changes in rat forebrain neurones. J Physiol. 1998; 509:103–116. [PubMed: 9547385]

27. Ben-Ari Y, Gho M. Long-lasting modification of the synaptic properties of rat CA3 hippocampal neurones induced by kainic acid. J Physiol. 1988; 404:365–384. [PubMed: 2908124]

28. Grabenstatter HL, Dudek FE. A new potential AED, carisbamate, substantially reduces spontaneous motor seizures in rats with kainate-induced epilepsy. Epilepsia. 2008; 49:1787–1794. [PubMed: 18494790]

29. Delorenzo RJ, Sun DA, Deshpande LS. Cellular mechanisms underlying acquired epilepsy: the calcium hypothesis of the induction and maintainance of epilepsy. Pharmacol Ther. 2005; 105:229–266. [PubMed: 15737406]

30. Pal S, Sombati S, Limbrick DD, et al. In vitro status epilepticus causes sustained elevation of intracellular calcium levels in hippocampal neurons. Brain Res. 1999; 851:20–31. [PubMed: 10642824]

31. Deshpande LS, Nagarkatti N, Ziobro JM, et al. Carisbamate prevents the development and expression of spontaneous recurrent epileptiform discharges and is neuroprotective in cultured hippocampal neurons. Epilepsia. 2008; 49:1795–1802. [PubMed: 18494784]

32. Hernandez-Fonseca K, Massieu L. Disruption of endoplasmic reticulum calcium stores is involved in neuronal death induced by glycolysis inhibition in cultured hippocampal neurons. J Neurosci Res. 2005; 82:196–205. [PubMed: 16175570]

33. Wang GJ, Thayer SA. Sequestration of glutamate-induced Ca2+ loads by mitochondria in cultured rat hippocampal neurons. J Neurophysiol. 1996; 76:1611–1621. [PubMed: 8890280]

34. Coulter DA, Huguenard JR, Prince DA. Characterization of ethosuximide reduction of low-threshold calcium current in thalamic neurons. Ann Neurol. 1989; 25:582–593. [PubMed: 2545161]

35. Coulter DA, Huguenard JR, Prince DA. Calcium currents in rat thalamocortical relay neurones: kinetic properties of the transient, low-threshold current. J Physiol. 1989; 414:587–604. [PubMed: 2607443]

36. Coulter DA, Huguenard JR, Prince DA. (1990) Differential effects of petit mal anticonvulsants and convulsants on thalamic neurones: calcium current reduction. Br J Pharmacol. 1990; 100:800–806. [PubMed: 2169941]

37. Zamponi GW, Striessnig J, Koschak A, et al. The Physiology, Pathology, and Pharmacology of Voltage-Gated Calcium Channels and Their Future Therapeutic Potential. Pharmacol Rev. 2015; 67:821–870. [PubMed: 26362469]

38. Zamponi GW. Targeting voltage-gated calcium channels in neurological and psychiatric diseases. Nat Rev Drug Discov. 2016; 15:19–34. [PubMed: 26542451]

39. Bialer M, Johannessen SI, Levy RH, et al. Progress report on new antiepileptic drugs: a summary of the Tenth Eilat Conference (EILAT X). Epilepsy Res. 2010; 92:89–124. [PubMed: 20970964]

Bullet Points

- Carisbamate (CRS) reversed kainic acid-induced elevations in intracellular calcium in CA3 pyramidal neurons

- CRS blocked epileptiform activity in hippocampal slices exposed to zero-Mg^{2+} or 4-AP

- CRS did not affect mitochondrial respiratory chain activity or Ca^{2+} release from the endoplasmic reticulum

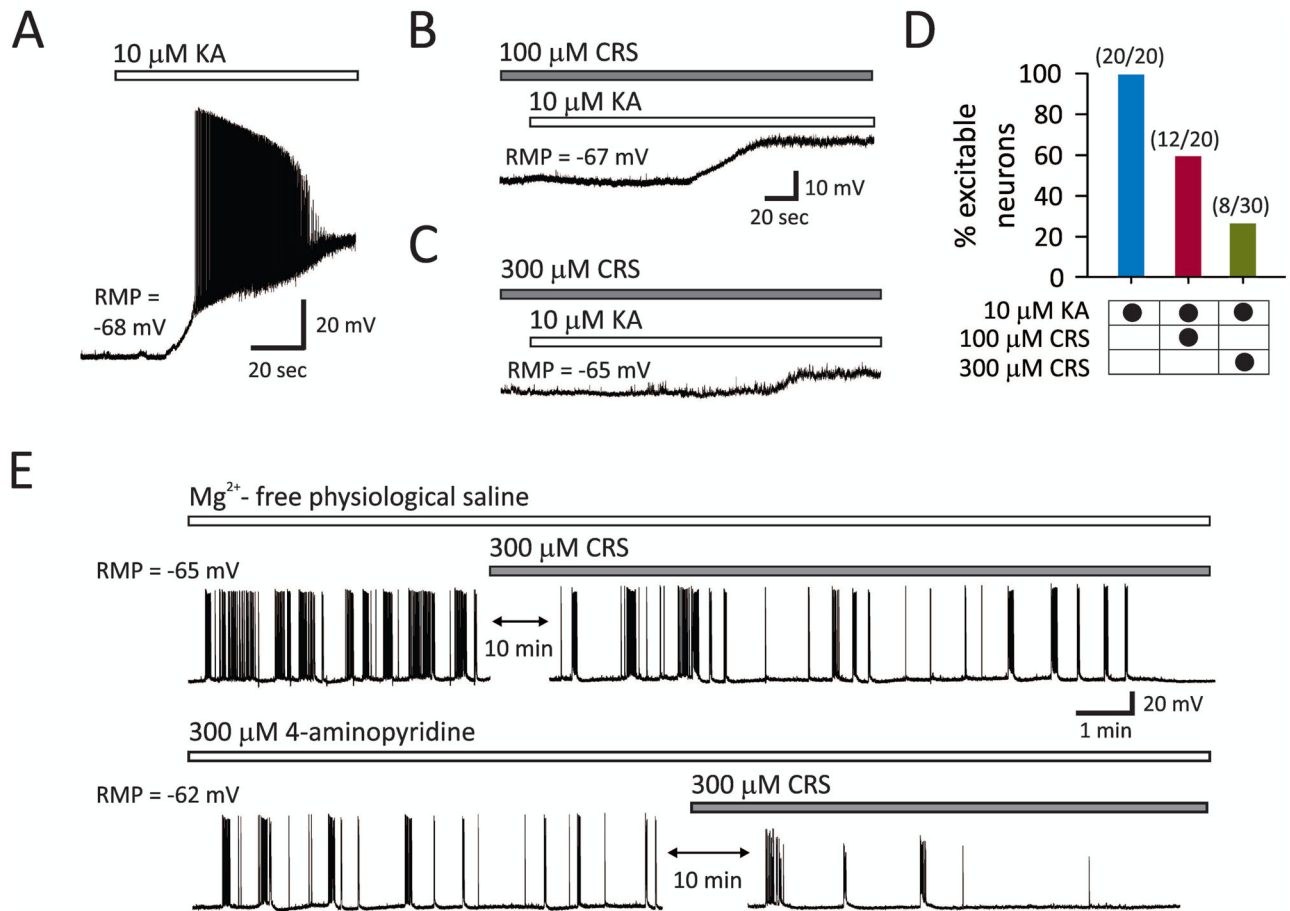- CRS decreased Ca^{2+} flux in HEK tsA-201 cells transfected with $Ca_v3.1$ voltage-dependent T-type Ca^{2+} channels

Figure 1. Effects of carisbamate (CRS) on epileptiform activity provoked under different conditions in vitro

(A) Bath application of 10 μM KA led to membrane depolarization and hyperexcitability of CA3 pyramidal neurons in acute hippocampal slices. (B, C) Pre-treatment with 100 μM CRS suppressed KA-induced neuronal hyperexcitability in 8 out of 20 cells, with the remainder being unaffected. Increasing CRS to 300 μM CRS led to 22 out of 30 cells being protected. (D) Summary of neuronal excitability changes following KA exposure alone, or with either 100 μM CRS or 300 μM CRS. Each vertical bar represents the percentage (%) of cells exhibiting neuronal hyperexcitability during combined KA and CRS application. (E) Representative traces depicting spontaneous "seizure-like" epileptiform activity beginning 30 min after continuous infusion of zero-Mg^{2+} physiological saline (*upper panel*) or perfusate containing 300 μM 4-aminopyridine (4-AP). Under both conditions, 300 μM CRS decreased epileptiform activity. RMP indicates resting membrane potential.
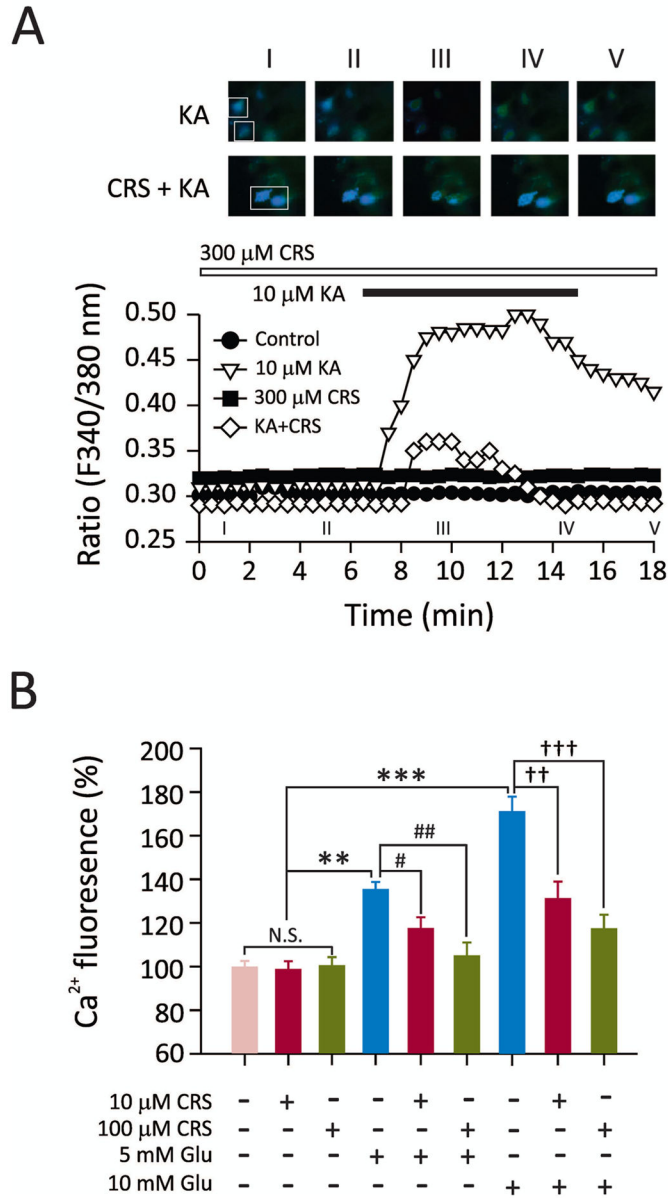
Figure 2. Effect of carisbamate (CRS) on calcium influx induced by either kainic acid (KA) or glutamate

(A) Following exposure to KA, the fluorescence ratio (at 340 and 380 nm excitation wavelengths; F340/380) increased dramatically in CA3 pyramidal neurons. While CRS alone did not alter the fluorescence signal, cells pre-treated with CRS showed a prominent reduction in calcium fluorescence intensity in the face of KA exposure. Photomicrograph series (I–V) at various time-points during KA and CRS challenge are shown, reflecting changes in $[Ca^{2+}]_i$ in pyramidal neurons as labeled with Fura2-AM; the white rectangles at time-point I depict Fura-2AM signals. (B) Changes in $[Ca^{2+}]_i$ load in HT-22 cells exposed to glutamate with or without CRS. Increases in $[Ca^{2+}]_i$ were seen following both 5 mM and 10 mM glutamate; these changes were attenuated in a dose-dependent manner by 10 μM and 100 μM of CRS. (*, compared to control cells *vs.* glutamate-treated cells; # compared to 5

mM glutamate-treated cells *vs.* 5 mM glutamate plus CRS-treated cells; † compared to 10 mM glutamate plus CRS-treated cells). CRS alone did not affect calcium accumulation. Values represent group means ± S.E.M. One-way ANOVA followed by Tukey test; **, $p <$ 0.01; ***, $p < 0.001$; #, $p < 0.05$; ##, $p < 0.01$; ††, $p < 0.01$; †††, $p < 0.001$.
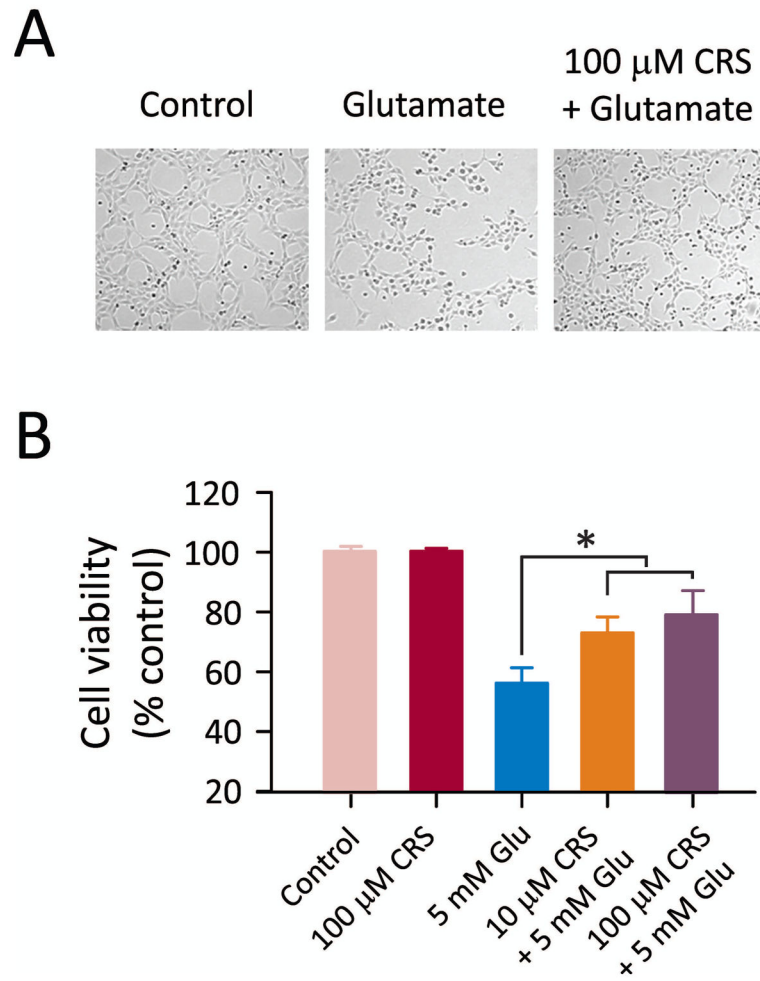
Figure 3. Carisbamate (CRS) is neuroprotective against glutamate-induced cell death
(A) Representative images of HT-22 cells 12 hr after administration with media alone
(control), 5 mM glutamate (Glu), and Glu plus 100 μM CRS. (B) Summary data of cell
viability using the MTT assay for various treatment groups. Glu alone produced over 40%
cell death and this effect was dose-dependently suppressed by CRS. Values represent group
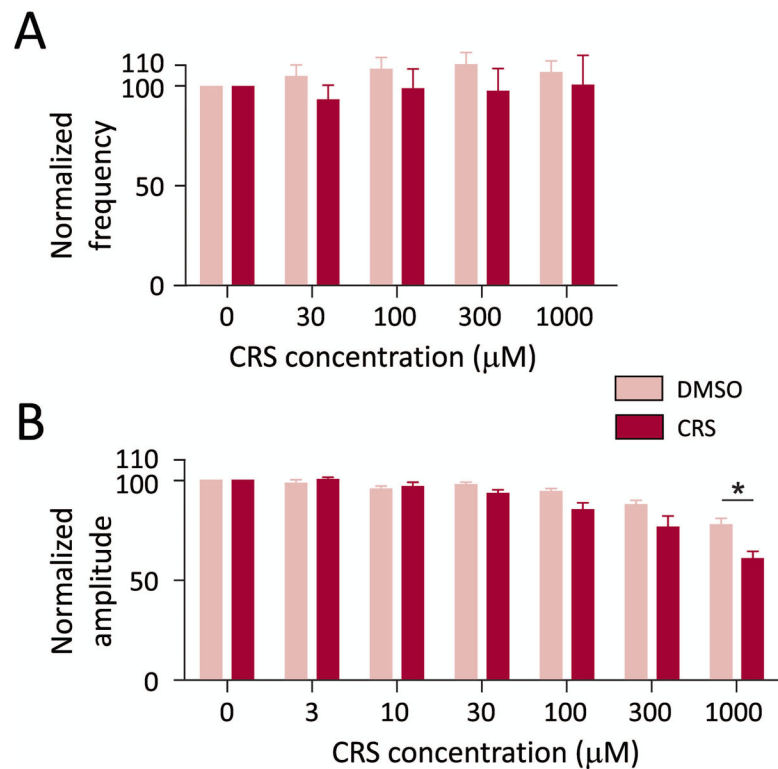means ± S.E.M. One-way ANOVA followed by Tukey test; *, $p < 0.05$.

Figure 4. Effect of carisbamate (CRS) on Store Overload-Induced Ca^{2+} Release (SOICR) in endoplasmic reticulum (ER)

Summary of single-cell fluorescence intensity measurements of SOICR with either DMSO (vehicle) alone or at various concentrations of CRS. (A) CRS did not significantly alter the frequency of store overload-evoked Ca^{2+} oscillations. (B) Despite a slight (but non-significant) reduction in the amplitude of store overload-evoked Ca^{2+} oscillations over the CRS dose range of 30–300 μM, no significant differences were seen. However, at 1 mM CRS, the amplitude of the store overload-evoked oscillations was significantly suppressed by CRS (student t-test; *, $p < 0.05$).
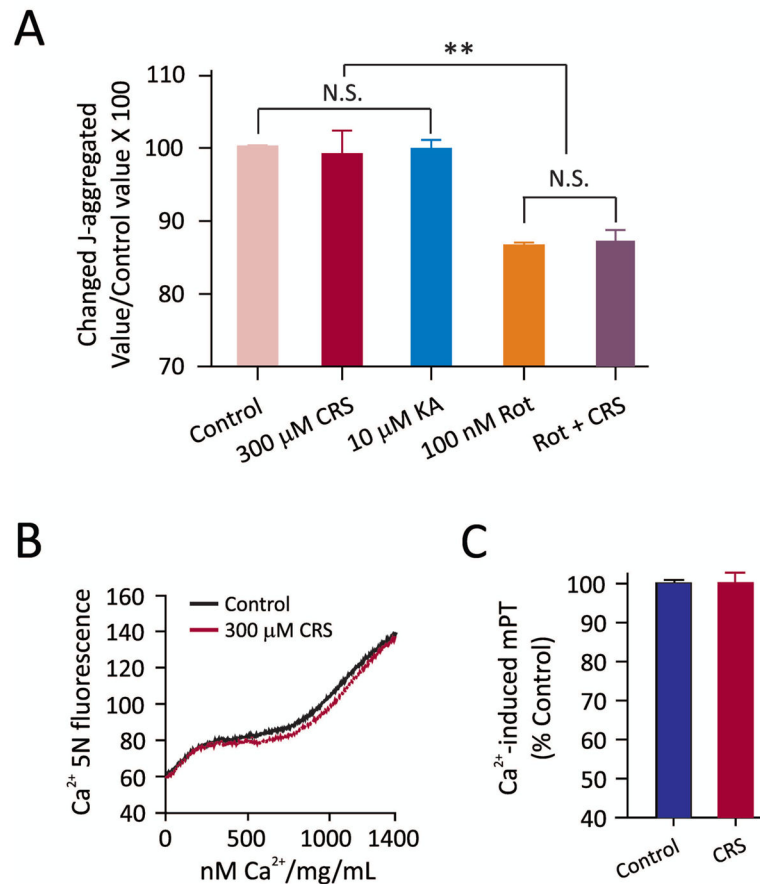
Figure 5. Effects of carisbamate (CRS) in acutely isolated hippocampal mitochondria
(A) No differences in the mitochondrial membrane potential (ψ) were seen with either 300 μM CRS or 10 μM KA. After the addition of 100 nM rotenone (Rot), ψ dissipated substantially but this action was not prevented by CRS. One way ANOVA followed by Tukey test; **, $p < 0.01$. (B, C) Representative traces and summary data depicting Ca^{2+}-induced mPT opening with and without CRS treatment. CRS (300 μM) did not affect mPT. Values represent mean ± S.E.M. Paired t-test was conducted between control *vs* CRS-treated groups.
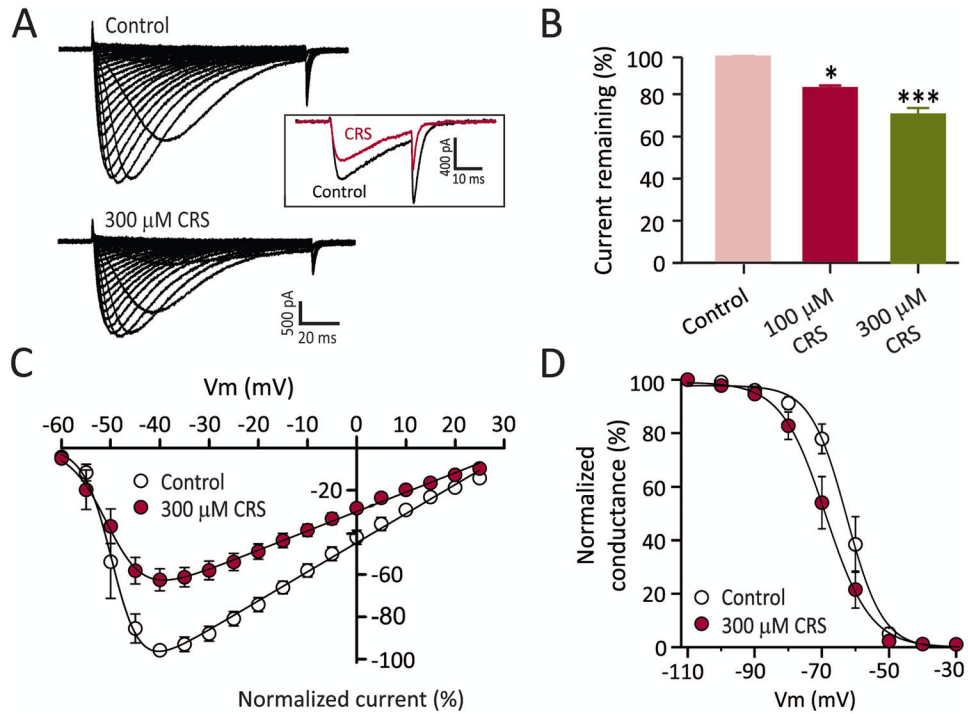
Figure 6. Effect of carisbamate (CRS) on cells transfected with Ca$_v$3.1 (T-type calcium) channels
(A) Representative traces showing Ca^{2+} currents recorded before and after bath application of 300 μM CRS. There is a significant decrease in the peak amplitude of the current in response to a depolarizing step up from −110 mV to −30 mV. The remaining Ca$_v$3.1 current was 83.2 ± 1.9% (p = 0.02, paired t-test, n = 6) and 71.2 ± 4.2% (p = 0.00003, paired t-test, n = 6) after application of CRS at 100 μM and 300 μM, respectively. (B) Bar graph summarizing the peak Ca^{2+} current amplitudes elicited with and without CRS (100 and 300 μM) treatment. (C) Current-voltage relationship for CRS block of Ca$_v$3.1. The half-activation potential from the fitted curves were −50.1 ± 0.4 mV and −51.2 ± 0.6 mV for before and after the application of CRS (300 μM, n = 6), p = 0.51 (paired t-test). (D) The steady-state inactivation curve for CRS block of Ca$_v$3.1. The half inactivation potential from the fitted curves were −62.6 ± 0.8 and −68.9 ± 1.0 for before and after the application of CRS (300 μM, n = 6), p = 0.0007 (paired t-test).